MAGNETS FOR MAGNETIC RESONANCE ANALYSIS AND IMAGING

Nuclear magnetic resonance (NMR) was discovered in 1946 by Purcell (1) and Bloch (2). Classically, it is the precession of the spins of nuclei with magnetic moment, subjected to a transverse radio frequency (RF) field in the presence of a longitudinal magnetic field. Nuclear species of biological interest having nonzero magnetic moment are listed in Table 1 together with their Larmor precession frequency-field dependence.

Table 1. The Larmor Precession Constant for Various Nuclides

Nuclide	Atomic Number	NMR Frequency (MHz/Tesla)
Hydrogen	1	42.5759
Deuterium	2	6.5357
Carbon	13	10.705
Oxygen	17	5.772
Sodium	23	11.262
Phosphorus	31	17.236

Experimentally, NMR is performed as follows (3,4): nuclei are immersed in a static field B_0, which results in the development of a net polarization along the field direction, occurring with a time constant τ_1. Transitions among their spin states are excited by a high-frequency field B_1, oriented perpendicular to the static field. In a rotating frame of reference (rotating at the Larmor precession frequency), the magnetization vector of the spin is tilted from a longitudinal direction (along B_0) toward the transverse plane. The angle of precession depends on the strength and duration of the applied RF field and is given by

$$\psi = \gamma B_1 \tau_\mathrm{p} \tag{1}$$

where τ_p is the pulse width and γ is the gyromagnetic ratio.

Following the pulse, the magnetization decays transversely with a time constant τ_2, the spin–spin relaxation time. The polarization develops (or decays) along the field with a time constant τ_1, the spin–lattice relaxation time.

NMR is the preeminent method for the identification of chemical species in weak solution. It also has useful applications in solid materials. The most exacting specifications for an NMR magnet are imposed by high-resolution NMR. The resonant frequency of a nucleus depends not only on B_0 but also, to a small extent, on the shielding provided by the electronic structure of the chemical compound. This effect is the chemical shift and is distinctive for each chemical species. Thus the resonant frequency of the ^{1}H nucleus in water is different from that in benzene (C_6H_6) or in the methyl or methylene group in alcohol (CH_3CH_2OH). These small differences in frequency are typically a few parts per million and provide a means to identify the components of a complex molecule.

Early NMR spectrometers used continuous wave (CW) methods in which the frequency of the B_1 field would be changed slowly and the absorption of a tank circuit enclosing the sample would be recorded as a spectrum of power absorption versus frequency. At the resonant frequency a sharp increase in absorption would be observed. The width of the peak depended, among other things, on the magnification Q of the tank circuit.

In modern NMR, a pulse of RF of sufficient strength and duration is applied to the sample so that all the spins are excited. The pulse is then switched off, and the signals emitted at various frequencies by the sample during relaxation of the spins are monitored. A Fourier analysis of the signal then transforms the time-dependent spectrum into a frequency-dependent signal, thus revealing the resonance peaks associated with the chemical shifts (3,4).

The uniformity of the static field B_0 is the key to high-resolution NMR and to sharp images in magnetic resonance imaging (MRI). A uniform field allows large numbers of nuclei to precess at exactly the same frequency, thus generating a strong signal of narrow bandwidth. The underlying theory and practice of high-homogeneity superconducting magnets is described in this section. MRI magnets differ from those used for NMR analysis in that spatial distribution of either signal strength or τ_1 or τ_2 relaxation times are measured over a volume far greater than that of a sample for chemical analysis. In MRI, the predominant nuclear species examined is hydrogen in water. Density or τ_1 or τ_2 is measured on planes throughout a body and reconstructed as two-dimensional maps.

The field strengths of NMR magnets are higher than those of MRI magnets. From the discovery of NMR, in 1946, to 1967, magnetic fields were limited to 2 T that could be generated by electromagnets. A 5 T superconducting magnet was introduced in 1967, and slow improvements led to the 20 T magnetic field available in NMR magnets today. The driving forces for the increase in field strength are the chemical shift (separation of the nuclear species which is linearly proportional to field strength), signal strength (which is proportional to the square of the field strength), and signal-to-noise ratio (which is proportional to the 3/2 power of the field strength). Although various experimental techniques have been applied to improve signal-to-noise ratio, including tailored pulse sequences, signal averaging, cooled conventional receiver coils and superconducting receiver coils, increased field strength is still desirable for increased chemical shift. Magnets for high-resolution NMR are now almost exclusively superconducting, and it is only that type that is described here.

The optimal field strength for MRI is determined by a number of factors, including reduction in imaging time, reduction in chemical shift artifacts, and reduction in cost, and by limits to the exposure of a patient to electromagnetic radiation, as set by regulations. Even though most MRI magnets have field strengths up to 1.5 T, a few experimental magnets have been built or designed for functional MRI studies with field strengths up to 8 T. In order to achieve the desired combination of field strength, working volume, and stability, superconducting magnets represent the principal type employed. However, both water-cooled resistive magnets, iron-cored electromagnets, and rare earth permanent magnet MRI systems have been used or are in use for special applications. The superconducting magnet is here considered exclusively.

DESIGN PRINCIPLES

NMR Magnets

The analysis of weak solutions imposes several requirements on the magnet. In order to obtain usable signal-to-noise ratios, a large volume of sample must be used. This immediately demands good field uniformity so that variations in background field strength do not give rise to different frequencies, which would, of course, mask the small chemical shifts being sought. High field strength is desired as detailed above. Even if these requirements are met, the dilution of the sample may be such that repeated pulses are required. The final signal-to-noise that can be obtained from a number of pulses is proportional to $\sqrt{N}$. A run may take many hours or even days to accomplish. During that time not only must the spatial homogeneity of the background field be excellent, but the magnitude of the field also must be constant, or at least must change only very slightly. (The reason that any change is permitted is that a frequency lock can be used to adjust the frequency of the RF to match a slow and slight change in the background field.)

To summarize, the NMR magnet should have high field strength and great uniformity, and the field must be stable.

MRI Magnets

The essential principles for MRI magnets are identical to those for NMR magnets, but the volumes of homogeneity are much greater, whereas the homogeneity is somewhat lower. Despite field strengths lower than those of NMR magnets, the stored magnetic energies of MRI magnets are greater by reason of the large bore, which must be sufficient to house correction coils, pulsed gradient coils, and a patient. The MRI system differs significantly from that of the NMR system by including means to superimpose linear field gradients on the background homogeneous field. These pulsed gradients define thin planes in which the field is known but different from that elsewhere. Thus the frequency of nuclear magnetic resonance is spatially encoded so that the signals generated by the relaxing nuclei have frequencies which define their position. As in NMR for chemical analysis, the MRI signals may interrogate either the density of nuclei or the τ_1 or τ_2 relaxation times.

THEORETICAL DESIGN

Almost all superconducting NMR and MRI magnets are solenoids. The reason for that is the relative simplicity and ease of manufacture and design of solenoids, compared with, for instance, extended dipoles. Although the generation of the RF field could be simpler with a transverse background field, the difficulty of manufacture of a high-background field magnet would far outweigh any advantage in the RF coil. The construction of a high-homogeneity solenoid proceeds in three parts: a winding array is designed, based solely on the analysis of the axial variation of the field of a solenoid; the magnet is wound and the spatial variation of its actual field is measured; and the unwanted errors in the field arising from manufacturing imperfections are removed by shimming.

The center field of a solenoid is given by

$$B_0 = \mu_0 J a_0 \ln\{[\alpha + (\alpha^2 + \beta^2)^{1/2}]/[1 + (1 + \beta^2)^{1/2}]\} \tag{2}$$

where J is the overall winding current density, a_0 is the inner radius, α is the ratio of outer to inner radii, and β is the ratio of length to inner diameter (5). Because SI units are used throughout, μ_0 is the permeability of free space, $4\pi \times 10^{-7}$ H/m, a_0 is in meters, and B_0 is in Tesla.

The field strength decreases at points on the axis away from the center of the solenoid. The axial variation of field strength on the z axis is expressible as a Taylor's series

$$\begin{aligned} B(z) = B_0 &+ (d^2B/dz^2)z^2/2 + (d^4B/dz^4)z^4/4! \\ &+ (d^6B/dz^6)z^6/6! + \cdots \end{aligned} \tag{3}$$

Only even terms appear because the center of the solenoid coincides with the origin.

Figure 1 illustrates the geometry of a thin solenoid, of radius a_0 and extending a length z_0 to the right of the origin. For such a thin solenoid, the derivatives of the field at the origin are as follows:

$$\begin{aligned} B_0 &= \tfrac{1}{2}\mu_0 i z_0 (a_0^2 + z_0^2)^{-1/2} \\ dB/dz &= -\tfrac{1}{2}\mu_0 i a_0^2 (a_0^2 + z_0^2)^{-3/2} \\ d^2B/dz^2 &= -\tfrac{1}{2}\mu_0 i 3 z_0 a_0^2 (a_0^2 + z_0^2)^{-5/2} \\ d^3B/dz^3 &= -\tfrac{1}{2}\mu_0 i a_0^2 (3a_0^2 - 12z_0^2)(a_0^2 + z_0^2)^{-7/2} \end{aligned} \tag{4}$$

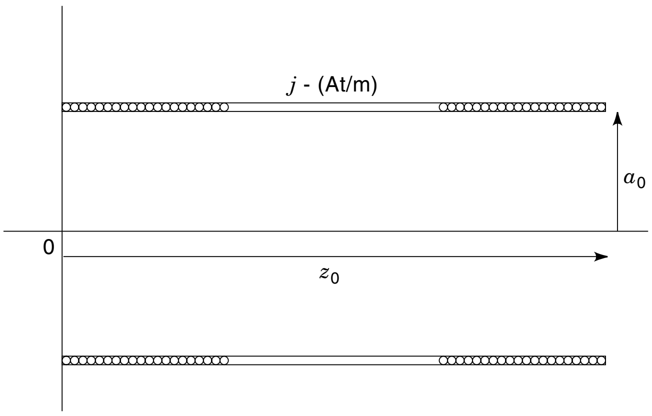

Figure 1. Geometry of a thin solenoid showing the coordinate system used to define current geometries.

where i is the sheet current density in amp-turns per meter and a_0 and z_0 are as illustrated in Fig. 1.

The field of a solenoid symmetric about the center plane has even symmetry and no odd derivatives. So, by evaluating the even derivatives of the field at the center, the axial variation of field generated by a solenoid can be calculated to an accuracy determined by the number of derivatives used and by the distance from the center. The derivatives can be treated as coefficients of a Cartesian harmonic series so that

$$B_z = B_0 + b_2 z^2 + b_4 z^4 + b_6 z^6 + \cdots$$

in which

$$\begin{aligned} b_2 &= \mu_0 i[3z_0 a_0^2 (a_0^2 + z_0^2)^{-5/2}]/4 \\ b_4 &= \mu_0 i[(45a_0^2 z - 60z^3)(a_0^2 + z_0^2)^{-9/2}]/48 \\ b_6 &= -\mu_0 i[(5a_0^4 z - 20a_0^2 z^3 + 8z^5)(a_0^2 + z_0^2)^{-13/2}]/1440 \end{aligned} \tag{5}$$

For coils of odd symmetry, such as shim coils described later, the corresponding harmonics are

$$\begin{aligned} b_1 &= \mu_0 i[(a_0^2 + z_0^2)^{-3/2}]/2 \\ b_3 &= \mu_0 i[(3a_0^2 - 12z^2)(a_0^2 + z_0^2)^{-7/2}]/12 \end{aligned} \tag{6}$$

Notice that the magnitude of any harmonic coefficient is mediated by the denominator of the expressions that each include the term $(a_0^2 + z_0^2)^{(n+1/2)}$, where n is the order of the harmonic. Thus, the generation of high-order harmonics requires coils with large values of current (ampere-turns) or small radius. This is significant in the construction of shim coils, as is noted later.

Associated with an axial variation of field is a radial variation, arising from radial terms in the solution of the Laplace scalar potential equation. For instance, even-order axial variations are accompanied by axisymmetric radial variations (6) of the form

$$\begin{aligned} B_2(z,x,y) &= b_2[z^2 - \tfrac{1}{2}(x^2 + y^2)] \\ B_4(z,x,y) &= b_4[z^4 - 3(x^2 + y^2) + \tfrac{3}{8}(x^2 + y^2)^2] \end{aligned} \tag{7}$$

These equations show that if b_2 or b_4 are zero there will be no axisymmetric radial variation of field.

Figure 2 illustrates a set of nested solenoids. Solenoid 1 gives rise to nonzero values of the harmonic coefficients b_2, b_4, b_6, etc. If dimensioned correctly, solenoid 2 by contrast can produce equal values for some or all these coefficients but with opposite polarity. Then at least b_2 and b_4 will have net zero values, and the first uncompensated harmonic to appear in the expression for axial field variation will be the sixth order. A minimum, but not necessarily sufficient, condition is that as many degrees of freedom are needed in the parameters of the coils as there are coefficients to be zeroed.

This method can be extended to as many orders as desired. In most high-resolution NMR magnets, the required uniformity of the field at the center is achieved by nulling all orders up to and including the sixth. That is, the solenoid is of eighth order. In the design of the solenoids, no odd order appears, of course. The first residual harmonic will have a very small value close to the center, although at greater axial distances, the field will begin to vary rapidly. Thus, the design of a high-homogeneity solenoid requires only the calculation of the field or the field harmonics on axis, and those harmonics may be easily calculated using only Cartesian coordinates.

MANUFACTURING ERRORS

The theoretical design of a high-homogeneity magnet can be simple because only axial terms in the z field need to be considered. However, the manufacturing process introduces errors in conductor placement which generate both even- and odd-order axial and, most significantly, radial field gradients. Further, the materials of the coil forms, the nonisotropic contraction of the forms and windings during cool-down to helium temperature and the effects of the large forces between the windings may also introduce inhomogeneity. Typically, the homogeneity of an as-wound set of NMR solenoids is not better than 10^{-5} over a 5 mm diameter spherical volume (dsv) at the center. For high-resolution NMR, an effective homogeneity of 10^{-9} over at least 5 mm dsv is required. The improvement of the raw homogeneity to this level is achieved by three steps, superconducting shim coils, room temperature shim coils and, in NMR magnets only, sample spinning. (Additionally, in cases of poor raw homogeneity, ferromagnetic shims may be used occasionally in NMR magnets and routinely in MRI magnets to compensate for large errors or significant high-order harmonics.) The presence of radial field gradients necessitates a more comprehensive field analysis than is convenient with Cartesian coordinates.

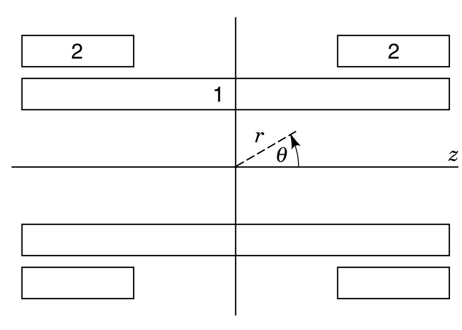

Figure 2. Principle of harmonic compensation. Coaxial solenoids generating field harmonics of opposite sign.

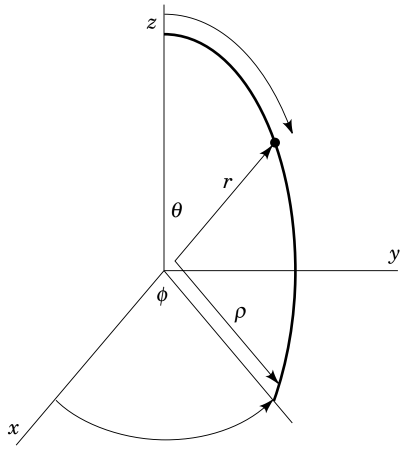

Figure 3. The system of spherical coordinates specifying field points and current sources.

LEGENDRE FUNCTIONS

The expression of the harmonics of the field in terms of Cartesian coordinates provides a simple insight into the source of the harmonics. However, as the order of the harmonic increases, the complexity of the Cartesian expressions renders manipulation very cumbersome, and an alternative method is needed. The Laplace equation for the magnetic field in free space is conveniently solved in spherical coordinates. These solutions are spherical harmonics, and they are valid only in the spherical region around the center of the solenoid, extending as far as, but not including, the nearest current element. Figure 3 illustrates the coordinate system for spherical harmonics. The convention followed here is that dimensions and angles without subscripts refer to a field point, and with subscripts they refer to a current source.

The axisymmetric z field generated by a coaxial circular current loop can be expressed in the form of a Legendre polynomial, thus,

$$B_z = \sum_{n=0}^{\infty} g_n r^n P_n(\cos\theta) \tag{8}$$

where r and θ define the azimuth of the field point in spherical coordinates, and u is $\cos(\theta)$. $P_n(u)$ is the zonal Legendre polynomial of order n and g_n is a generation function given by

$$g_n = \mu_0 i P_{n+1} \cos(\theta_0)\sin(\theta_0)/(2\rho^{n+1}) \tag{9}$$

where θ_0 and ρ_0 define the position of the current loop in spherical coordinates. In this text, it is the convention that $n = 0$ represents a uniform field. The field strength given by Eqs. (8) and (9) is constant with azimuth at constant radius r.

Equations (8) and (9) are equivalent in spherical coordinates to those of Eqs. (4), (5), and (7) on the z axis but additionally predict the z field off axis. In the design of the main coils Eqs. (8) and (9) offer no more information than Eq. (5). However, in the calculation of the off-axis z fields, they provide important additional information that can be used in the optimization of coil design when fringing fields must be considered.

The harmonic components of the z field can also be expressed in the form of associated Legendre functions of order n, m (7). Those functions define the variation of the local z field strength at points around the center of the magnet and include variation of the field with azimuth φ. Thus,

$$B_z(n, m) = r^n(n+m+1)P_{n,m}(u) \times [C_{n,m}\cos(m\varphi) + S_{n,m}\sin(m\varphi)] \tag{10}$$

where $C_{n,m}$ and $S_{n,m}$ are the harmonic field constants in tesla per meter^n, $P_{n,m}(u)$ is the associated Legendre function of order n and degree m, and u is $\cos(\theta)$. The order n is zonal, describing the axial variation of z field. The degree m is tesseral, describing the variation of the z field in what would be the x–y plane in Cartesian coordinates. φ is the azimuth to the point at radius r from an x–z plane. θ is the elevation of the point from the z axis. Tables of the values of the Legendre polynomials can be found in standard texts on mathematical functions (8).

In Eq. (10), m can never be greater than n. For example, if $n = m = 0$, $B_z(0,0)$ is a uniform field independent of position. If $n = 2$ and $m = 0$, $B_z(2,0)$ is a field whose strength varies as the square of the axial distance [i.e., B_2 of Eq. (7)]. If $n = 2$ and $m = 2$, $B_z(2,2)$ is a field that is constant in the axial direction but increases linearly in two of the orthogonal radial directions and decreases linearly in the other two. Figure 4 shows a map of the contours of constant field strength of a $B_z(2,2)$ field harmonic for which $S_{2,2} = 0$. The $B_z(2,2)$ field has zero magnitude at the origin and along the x and y coordinate axes. Of course, the direction of the zero values of the $B_z(2,2)$ harmonic will not generally lie in the Cartesian x and y planes. Depending on the relative values of $C_{n,m}$ and $S_{n,m}$ in Eq. (10), the zero harmonic planes will lie at an angle other than $\phi = 0$ or $m\pi/2$. The constant field contours of $B_z(2,2)$ extend to infinity along the z axis and represent, arbitrarily in this figure, values for $B_z(2,2)$ of 10^{-4}, 10^{-6}, and 10^{-8}, for example. Within the indicated cylinder centered on the z axis, the value of the harmonic is everywhere less than 10^{-6}. For

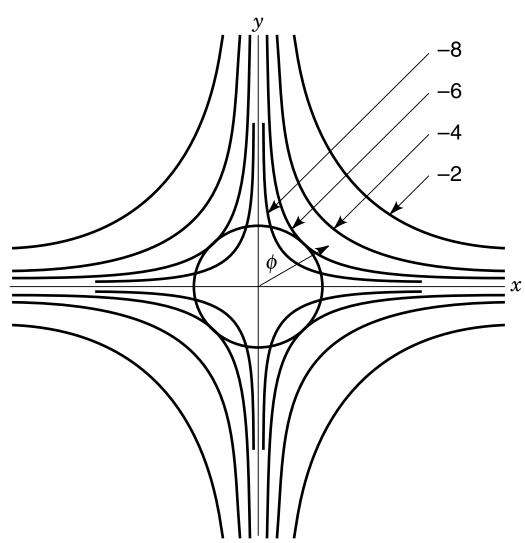

Figure 4. Surfaces of constant magnitude of a $B(2,2)$ harmonic field, showing that the tesseral harmonic is zero when the azimuth ϕ is a multiple of $\pi/2$.

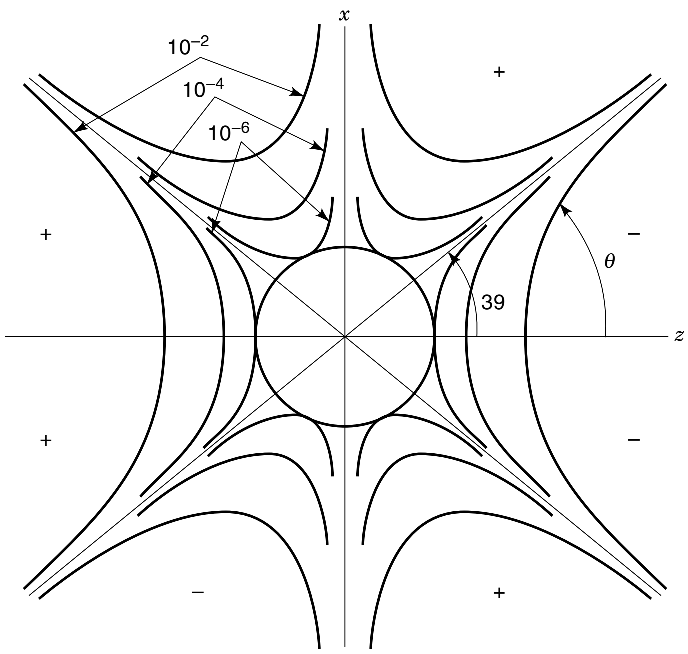

Figure 5. Surfaces of constant magnitude of a $B(3,0)$ harmonic field, showing that the zonal harmonic is zero when the elevation μ is 39° or 90°.

higher values of m, there are more planes of zero value. Thus, $B_z(4,4)$ has eight planes of zero value, $B_z(8,8)$ has 16, and so forth. A harmonic $B_z(4,2)$ defines a field in which the second-degree azimuthal variation itself varies in second order with axial distance.

The zonal harmonics $B_z(2,0)$, $B_z(3,0)$, $B_z(4,0)$ have conical surfaces on which the value of the field is zero. Thus, for instance, $B_z(3,0)$ has contours of zero value such as are shown in Fig. 5 to lie at $\theta = 39°$ and 90°.

The four hyperbolas are actually surfaces of rotation about the z axis, and each represents a constant value for $B_z(3,0)$ of, say, 10^{-6} [the uniform field, $B_z(0,0)$ at the origin having unity value]. Within the indicated ellipsoid, centered on the origin, the value of the $B_z(3,0)$ harmonic is therefore everywhere less than 10^{-6}.

The contours of the zero values of the spherical harmonics are analogous to combinations of Figs. 4 and Fig. 5. The zero values now lie on straight lines radiating from the origin. The surfaces of constant value look like the spines of sea urchins. As for the zonal harmonics, ellipsoidal surfaces roughly describe boundaries within which the magnitudes of the spherical harmonics do not exceed a given value. These error surface diagrams are often used in the design of an MRI magnet to identify the maximum calculated field error within a central volume caused by the highest uncompensated harmonic.

Thus, in general, the deviations from the ideal uniform solenoidal field can be expressed as the sum of a large number of harmonics each described by the associated Legendre function of order n and degree m. Although the Cartesian expressions of Eq. (4) can be used for the design of a coil system to generate a uniform field, the associated Legendre functions must generally be used for the analysis of the measured field and the design of shim coils or of ferromagnetic shims to compensate for harmonics with nonzero values of m (9).

Optimization Methods

With the recent rapid increase in the speed and size of computers, an alternative technique for the design of uniform field magnets has been developed. Not only is a uniform field of specific magnitude required but that should be combined with other criteria. For instance it could be accompanied by the smallest magnet, that is, the minimum of conductor, or by a specified small fringing field. To achieve these ideal solutions, an optimization technique is now generally used. The field strength of a set of coils is computed at points along the axis, and, if fringing field is a consideration, at points outside the immediate vicinity of the system. The starting point may be a coil set determined by a harmonic analysis as described earlier. Now however, mathematical programming methods are employed to minimize the volume of the windings satisfying the requirement that the field should not vary by more than the target homogeneity for each of the chosen points. Again, for purposes of homogeneity, only field on axis is considered because the radial variation of axisymmetric components of field is zero if the axial component is zero. The field strengths at points outside the magnet will be minimized by inclusion of a set of coils of much larger diameter than the main coils but carrying current of reverse polarity.

All design techniques, but particularly that of optimization, are complicated by the highly nonlinear relationship between the harmonic components generated by a coil and the characteristics of the coil. Thus the reversal in sign of the harmonic components occurs rapidly as the dimensions or position of a coil are changed. In the example of an NMR magnet shown in Fig. 6, the value of the second harmonic changes by 4 ppm for an increase in the diameter of the wire in the small coil "l" of only 0.1 mm. The optimization of the ampere-turns, shape and position of a coil thus affects the various harmonics in highly nonlinear and often conflicting ways.

Design optimization involves the computation of an objective function which contains all the elements that have to be minimized, subject to a set of constraints (10). For example, it may be required to minimize some combination of winding volume or magnet length subject to constraints on the field error at a number of points within the bore and on the fringing field at some point outside the magnet. The objective function would then be of the form

$$\sum_{i=1}^{N} pV_i + L \tag{11}$$

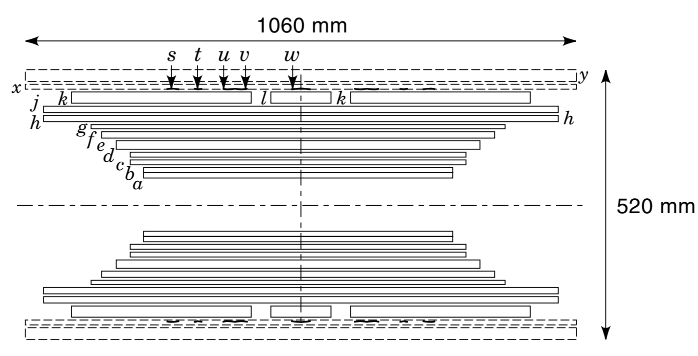

Figure 6. Coil profiles of an actual 8th order compensated NMR solenoid. The graded sections a through j produce axial harmonics of which orders 2, 4, and 6 are compensated by sections k and l. Layers x and y are shim coils.

where V_i is the volume of a coil, N is the number of coils, and L is the length of the magnet. The factor p weights the relative importance of the volume and of the length. This objective function is then minimized subject to the following constraints:

$$\left[\sum_{i=1}^{N} B_{i,p} - B_0\right]^2 < \Delta B^2 \tag{12}$$

$$\sum_{i=1}^{N} B_{i,f} < B_f \tag{13}$$

In Eq. (12) $B_{i,p}$ is the field at point p due to coil i. The equation represents the constraint on uniformity of field. It could also be expressed in terms of harmonic terms; for example, each even term up to $P_{10,0}$ being less than 10^{-6} B_0, the center field. [The inclusion of the squared terms in Eq. (12) allows for either positive or negative error field components.] Equation (13) expresses the condition that the fringing field should be less than, say, 1 mT (10 gauss) at a point, outside the magnet system. The 10 gauss criterion frequently represents the maximum field to which the public may be exposed in accessible areas around an MRI system.

The minimization of the objective function is performed by a mathematical programming algorithm, whereas the solution of the constraining Eqs. (12) and (13) will require a nonlinear technique (such as Newton–Raphson), in order to deal with the extremely nonlinear variation of the harmonics as they change with coil geometry (11).

SHIELDING

The minimization of the external fringing field is becoming increasingly important for the siting of MRI systems, so the active shielding of MRI magnets with center fields up to 2 T is now almost universal. (Active shielding of MRI magnets with center fields above 2 T is uneconomical and is not generally attempted.) Active shielding is generally achieved by the inclusion in the coil array of two reverse polarity coils at diameters typically twice that of the main coils. Because of the large dipole moment of an MRI magnet, the unshielded fringing field will extend several meters from the boundary of the cryostat. Consequently, active shielding is applied to many MRI magnets with central fields of over 0.5 T (12). The effect of the shielding on the harmonics of the center field must, of course, be included in the design of the compensation coils.

SHIMMING

The harmonic errors in the field of an as-built magnet divide into purely axial variations (axisymmetric zonal harmonics, which are accompanied by radial variations dependent on the elevation θ from the z axis, but independent of ϕ) and radial variations (tesseral harmonics, which depend on ϕ, where ϕ is the angle of azimuth in the x–y plane).

In order to compensate for the presence of various unwanted harmonic errors in the center field of the as-built coils, additional coils capable of generating the opposite harmonics are applied to the magnet. For each set of n and m in the associated Legendre functions, a current array can be designed in the form of a set of arcs of varying azimuthal extent and symmetry and with various positions and extents along the z axis. The magnitude of the harmonic field that an array generates can be controlled by the current. This is the principle of variable harmonic correction for both MRI and NMR magnets. (Correction by means of ferromagnetic shims is not variable.)

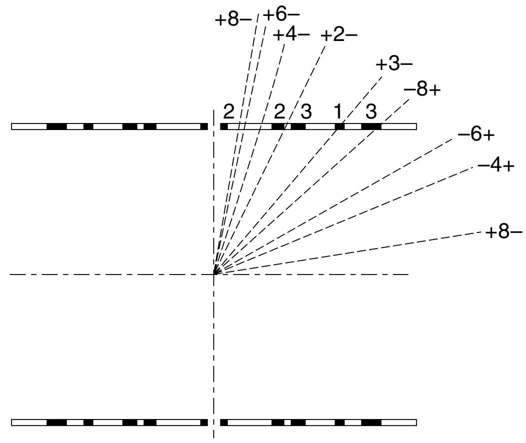

Figure 7. A set of axial shim coils for harmonic correction up to $B(3,0)$. These coils generate small harmonics of 4th order and higher.

The shimming of the unwanted harmonics is a process in two independent parts. First, there is the design of as many sets of coils as are needed to generate the compensating harmonics. Second is the measurement of the actual field errors to determine the magnitudes of the various harmonic components and the application of currents to the previously designed coils to provide the compensation. In fact, because superconducting shims must be built into the magnet prior to installation in the cryostat and cooldown, the range of harmonic errors in the field of the as-built magnet must be largely anticipated. Typically it might be assumed that the level of harmonic error decreases by a factor of three for each unit increase in n or m. Therefore, as a rough guide it has been found that compensation of up to $B(3,0)$ for the zonal harmonics and up to $B(2,2)$ for the tesseral harmonics is satisfactory in most cases for the superconducting shims of small bore NMR magnets. There will also be a set of room temperature shims in a high resolution NMR system. Those will compensate for errors typically up to $B(6,0)$ and $B(3,3)$ in many cases. Typically there may be up to 28, but exceptionally up to 45 independent shims in all. They will be constructed according to a different principle from the superconducting shims. The shimming of MRI magnets is accomplished by current shims, typically up to $n = 3$ and $m = 2$, and by ferromagnetic shims.

Superconducting Axial Shims

These will be simple circular coils combined in groups so as to generate a single harmonic only (13). Thus, a coil to generate $B(3,0)$ must generate no $B(1,0)$ nor $B(5,0)$. Because the superconducting shim coils need to generate only a small fraction of the field due to the main coil, they generally need only comprise one to three layers of conductor. For that reason the harmonic sensitivities can be calculated directly from Eqs. (4) and (5). A set of axial shims providing correction of $B(n,0)$ harmonics for $n = 1$ through 3 are shown in Fig. 7. Note that, for a fixed linear current density, only the angles defining the start and end of each coil are needed, together, of course, with the current polarities, either side of the center plane of the magnet, odd for $n = 1, 3, 5, \ldots$ and even for $2, 4, 6, \ldots$.

The set of coils illustrated in Fig. 7 generate negligible harmonics above the third order, $B(3,0)$. The individual coils of each harmonic group are connected in series in sets, there being in each set enough coils to generate the required axial harmonic but excluding, as far as is practical, those harmonics that are unwanted. Thus, in the figure, coils labeled 2 generate second-order $B(2,0)$ but no fourth order. However, they do generate higher orders. The first unwanted order is $B(6,0)$ but that is small enough that it may be neglected. So also with all higher orders because the denominator in the expressions of Eqs. (4) and (5) strongly controls the magnitude of the harmonic. Also illustrated in the figure is the effect on harmonic generation of the angular position of a circular current loop. Each of the dashed lines lies at the zero position of an axial harmonic. Thus, at an angle of 70.1° from the z axis, the $B(4,0)$ harmonic of a single loop is zero. Two loops carrying currents of the same polarity and suitable magnitude may be located on either side of the 70.1° line to generate no fourth-order harmonic yet generate a significant second order harmonic. Similarly, a coil for the generation of only a first order axial harmonic is located on the line for zero third order. The zero first-order harmonic line is at 90°, the plane of symmetry. In order therefore to generate a third order with no first, two coils must be used, with opposing polarities. The coils are all mirrored about the plane of symmetry, but the current symmetries are odd for the odd harmonics and even for the even harmonics. The loops may be extended axially as multiturn coils while retaining the property of generating no axial harmonic of a chosen order, if the start and end angles subtended by the coils at the origin are suitably chosen.

The principles described earlier can be applied both in the design of shim coils and in the selection of main coil sets. A further observation from the zero harmonic lines of Fig. 7 is that the higher harmonics reverse sign at angles close to the plane of symmetry of the system. This implies that, to produce single, high-order harmonics, coil positions close to the plane of symmetry must be chosen because the other coil locations where the sign of the harmonic reverses are too far from the plane of symmetry to be usable; the coils lying a long way from the plane of symmetry generate weak high-order harmonics.

Superconducting Radial Shims

The radial shims are more complex than those for purely axial harmonics because the finite value of m requires a $2m$-fold symmetry in the azimuthal distribution of current arcs, the polarity of current always reversing between juxtaposed arcs in one z plane (6,9). For instance, $m = 2$ requires four arcs, as shown in Fig. 8. However, as for $m = 0$, the set of current arcs shown in Fig. 8 will generate $B(n,m)$, where n is 2, 4, 6, etc., or 1, 3, 5, etc., depending on even or odd current symmetry about the $z = 0$ plane. So, the positioning of the arcs along the z axis is again crucial to the elimination of at least one unwanted order, n. Fortunately, the azimuthal symmetry generates unique values of the fundamental radial harmonic m. (Eight equal arcs cannot generate an $m = 2$ harmonic.) However, depending on the length of the arc, higher radial harmonics may be generated. For the shim coil configuration of Fig. 8, the first unwanted radial harmonic is $m = 6$. The higher tesseral harmonics are much smaller than the fundamental because of the presence in the expression for the field of a term $(r/r_0)^n$. Generally, the arc length is chosen to eliminate the first higher-degree radial harmonic. As an example, if the arc length of each shim coil shown in Fig. 8 is 90° the $B(6,6)$ harmonic disappears. The $B(10,10)$ harmonic is negligible.

The superconducting shims are almost invariably placed around the outside of the main windings. Although the large radius reduces the effective strength of the harmonics they generate, the shim windings cannot usually be placed nearer to the center of the coil because of the value of winding space near the inner parts of the coil and because of the low critical current density of wires in that region due to the high field. A comprehensive treatment of shim coil design may be found in Refs. 6 and 9. Those references also include details of superconducting coil construction. It should be noted, however, that some expressions in Ref. 6 contain errors.

Ferromagnetic Shims

Ferromagnetic shimming is occasionally used in high field, small bore NMR magnets, but its principal use is in MRI magnets. It is in that application that it will be described. The principle invoked in this kind of shimming is different from that of shim coils. The shims now take the form of discrete pieces of ferromagnetic material placed in the bore of the magnet. Each piece of steel is subjected to an axial magnetizing field at its position sufficient to saturate it. It then generates a field at a point in space that is a function of the mass of the shim and its saturation magnetization B_s with little dependence on its shape. For ease of example, a solid cylinder of steel will be assumed. The axis of the cylinder is in line with the field, as shown in Fig. 9. (In Fig. 9 the axis labeled z is that of the shim, not that of the MRI magnet itself. In fact, the shim will usually be placed at the inside surface of the bore of the MRI magnet.)

The field B, caused by the ferromagnetic shim, contains both axial and radial components. The axial component B_z is the correcting field required, and it adds arithmetically to the field of the magnet. The radial component adds vectorially to the field and produces negligible change in the magnitude of

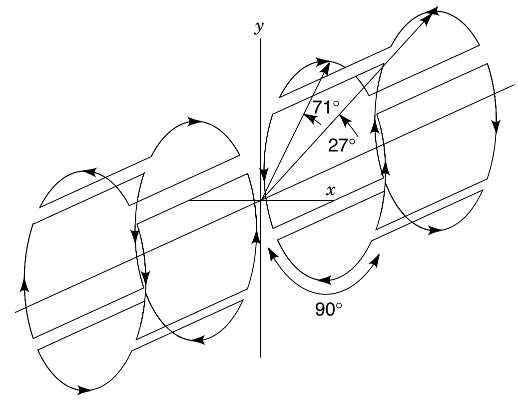

Figure 8. Schematic of a set of radial shim coils for correction of a $B(2,2)$ harmonic showing the positioning necessary to eliminate $B(4,2)$ and $B(4,4)$.

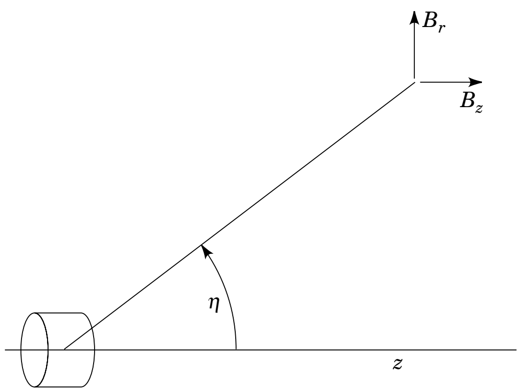

Figure 9. Field vectors generated by a ferromagnetic shim in the bore of an MRI magnet. B_z adds arithmetically to the main field; B_r adds vectorially and so has negligible influence on the field.

the axial field. Therefore, only the axial component of the shim field must be calculated. If the saturation flux density of the shim is B_s, the axial shim field is given by

$$B_z = B_s V[(2 - \tan^2\eta)/(\tan^2\eta + 1)^{5/2}]/(4\pi z^3) \qquad (14)$$

where V is the volume of the shim and z and η are as shown in Fig. 9.

The practical application of ferromagnetic shims involves the measurement of the error fields at a number of points, and the computation of an influence matrix of the shim fields at the same points. The required volumes (or masses) of the shims are then determined by the inversion of a U, W matrix, where U is the number of field points and W is the number of shims. In an MRI magnet, the shims are steel washers (or equivalent) bolted to rails on the inside of the room temperature bore of the cryostat. In the occasional ferromagnetic shimming of an NMR magnet, the shims are coupons of a magnetic foil pasted over the surface of a nonmagnetic tube inserted into the room temperature bore or, if the cryogenic arrangements allow, onto the thermal shield or helium bore tube. As in the design of the magnet, linear programming can be used to optimize the mass and positions of the ferromagnetic shims (e.g., to minimize the mass of material).

Resistive Electrical Shims

The field of an NMR magnet for high resolution spectroscopy must be shimmed to at least 10^{-9} over volumes as large as a 10 mm diameter cylinder of 20 mm length. If, as is usually the case, substantial inhomogeneity arises from high-order harmonics (n and m greater than 3), superconducting shims are of barely sufficient strength. This arises because of the large radius at which they are located, at least in NMR magnets (e.g., in the regions x and y of Fig. 6). In general, the magnitude of a harmonic component of field generated by a current element is given by

$$B_n \propto r^{n+1}/r_0^{n+1} \qquad (15)$$

where r is the radius vector of the field point, and ρ_0 is the radius vector of the source. Thus, the effectiveness of a remote source is small for large n.

In order to generate useful harmonic corrections in NMR magnets for large n and m, electrical shims are located in the warm bore of the cryostat. Although in older systems those electrical shims took the form of coils tailored to specific harmonics, modern systems use matrix shims. Essentially, the matrix shim set consists of a large number of small saddle coils mounted on the surface of a cylinder. The fields generated by unit current in each of these coils form an influence matrix, similar to that of a set of steel shims. The influence matrix may be either the fields produced at a set of points within the magnet bore, or it may be the set of spherical harmonics produced by appropriate sets of the coils.

FIELD MEASUREMENT

The accurate measurement of the spatial distribution of field in the as-wound magnet is essential to shimming to high homogeneity. Sometimes, measurement of the field is possible at very low field strengths with tiny currents flowing in the windings at room temperature. That may allow mechanical adjustment of the positions of the main compensations coils ($k - k$ in Fig. 6) to reduce the B(1,0), B(2,0) and B(1,1) harmonics. Major field measurement is made with the magnet at design field strength and in persistent mode. The methods of measurement in NMR and MRI magnets are generally different.

In NMR magnets, because of the small bore, the field is measured by a small NMR probe on the surface of a cylindrical region about 8 mm diameter and over a length of up to 10 mm. The measurements are made at typically 20° azimuthal intervals. From these field measurements, the predominant harmonics can be deduced, using a least-squares fit, and shimmed by means of the superconducting shim coils, both axial and radial. With subsequent measurements, as the harmonic content becomes smaller, the higher harmonics become evident and in turn can be shimmed. The field measurements are usually reduced to harmonic values because the shim sets are designed to generate specific harmonics. The correcting current required in any particular shim set is then immediately determined. Measurement and shimming is always an iterative process, generally requiring several iterations to achieve homogeneities of better than 10^{-9} over 5 mm dsv.

Field measurement in an MRI magnet is usually performed differently because much more space is available and because knowledge of the magnitudes of the harmonics in associated Legendre polynomial form is an advantage in the shimming process. In this case, the measuring points will lie on the surface of a sphere. Typically, the diameter of this sphere may be 500 mm. The field is measured at intervals of ϕ, often 30°, around each of the circles of intersection with this spherical surface of several z = const planes, called Gauss planes. From these measurements and by the property of orthogonality of the associated Legendre functions, the values of the constants $C_{n,m}$ and $S_{n,m}$ in Eq. (10) can be deduced by the following methodology.

The double integral

$$\int_{-1}^{+1}\int_{0}^{2\pi} P(n,m)(u)[\cos(m\phi)]P_{i,j}(u)[\cos(j\phi)]\,du.d\phi$$

is nonzero only if $i = n$ and $j = m$. Then, for $m > 0$, its value is

$$2\pi(n+m)!/(2n+1)(n-m)!$$

So, if both sides of Eq. (10) are multiplied by $P_{i,j}(u)[\cos(j\phi)]$ or $P_{i,j}(u)[\sin(j\phi)]$ and double integrated, the right-hand side will be nonzero only if $i = n$ and $j = m$. Then

$$\int_{-1}^{+1}\int_{0}^{2\pi} B_z(n,m)P_{i,j}(u)[\cos(j\phi)]\,du.d\phi = C_{n,m}r^n(n+m+1)2\pi(n+m)!/(2n+1)(n-m)!$$

and

$$\int_{-1}^{+1}\int_{0}^{2\pi} B_z(n,m)P_{i,j}(u)[\sin(j\phi)]\,du.d\phi = S_{n,m}r^n(n+m+1)2\pi(n+m)!/(2n+1)(n-m)! \quad (16)$$

Equation (16) are realized in practice by the measurement of the field at each of 60 points (for example) and the multiplication of each value by the spherical harmonics, $P_{i,j}(u)\cos(j\phi)$ and $P_{i,j}(u)\sin(j\phi)$ at that point. The integration is numerical. The method usually employed is Gaussian quadrature, similar in principle to Simpson's rule for numerical integration in Cartesian coordinates, but in which the z = const planes are the roots of the Legendre polynomial and the weights assigned to the values measured on each of these planes are derived from the Lagrangian. Tables of the roots and weights are found in standard texts on numerical analysis (14). For the purposes of example, assume the number of planes $p = 5$, and the number of azimuthal points per plane $q = 12$, for a total of 60 points on the surface. The planes are at $z/r = 0$, $z/r = \pm 0.5385$, and $z/r = \pm 0.9062$; r is the radius of the spherical surface. The corresponding weights are 0.5689, 0.4786, and 0.2369. The measurements are made on the circles of intersection and two numerical integrations of Eq. (16) performed, one for the $\cos(m\phi_\theta)$ terms and the other for the $\sin(m\phi_\theta)$ terms. Then the values of $C_{n,m}$ and $S_{n,m}$ are obtained from

$$C_{n,m} = \left[\sum_{p}^{p}\sum_{q}^{q} w_q B(u_p,\phi_q)P_{n,m}(u_p)\cos(m\phi_\theta)\right] \times [(2n+1)(n-m)!]/[2\pi r^n(n+m+1)!] \quad (17)$$

$$S_{n,m} = \left[\sum\sum w_q B(u_p,\phi_q)P_{n,m}(u_p)\sin(m\phi_\theta)\right] \times [(2n+1)(n-m)!]/[2\pi r^n(n+m+1)!] \quad (18)$$

where $B(u_p, \phi_q)$ is the field at the point p, q, the subscripts p and q denote each of the 60 points, and w_q is the Gaussian weighting for the plane q.

NMR MAGNET DESIGN AND CONSTRUCTION

Practical issues peculiar to the design and construction of NMR magnets include the following:

The wire diameter must be such that layers of windings near the inner radius of the solenoids do not generate discrete field fluctuation of a size comparable to the desired homogeneity. For example, if the wire diameter is very large, say, greater than 3 mm, the field will develop a fine structure away from the z axis. If the winding lay of a large diameter wire is helical in each layer, a helical structure may arise in the amplitude of the field with consequent problems in the correction of the resulting high harmonics.

Nonmagnetic coil forms must be used because the presence of discrete regions of ferro- or strong paramagnetism will generate large harmonics of high order (large n and possibly also m), which would be very difficult to shim.

The index of the wire must be high. All high-resolution NMR requires high field stability, with a decay not exceeding about 10^{-8} per hour. To achieve that, the magnets operate in persistent mode. A superconducting switch is closed across the winding after energization so that the current flows without loss in a resistanceless circuit. The superconducting switch consists of a small coil (usually noninductive) of a superconducting wire equipped with a resistance heater. When the heater is energized, the temperature of the coil is raised above the critical value, and the coil becomes resisitive. The charging voltage applied to the magnet then causes only a small current to flow in the switch. When the magnet has been charged, the switch heater is turned off, the coil cools, and the magnet current can then flow through the switch without loss. If a magnet does not need frequent resetting, its rate of field decay must be small. The joints between wire lengths and the switch and the magnet must be superconducting, and the wire must be without resistance. Although the joints can indeed be made so that their critical currents exceed the operating current, the effective resistance of the wire, owing to its index, may be high enough that decay in persistent mode exceeds acceptable levels for NMR. The resistance of the wire, manifest as a low value of the index, arises from variation in the critical current along the length of the wire. If a short region exists where the superconducting filaments are thin or have low pinning strength, a fraction of the current transfers between superconducting filaments through the copper (or bronze) matrix, giving rise to the resistance. The voltage associated with this resistance appears in critical current measurements on samples of the wire.

Figure 10 shows the typical trace of voltage gradient along a superconducting wire in a fixed field as a function of cur-

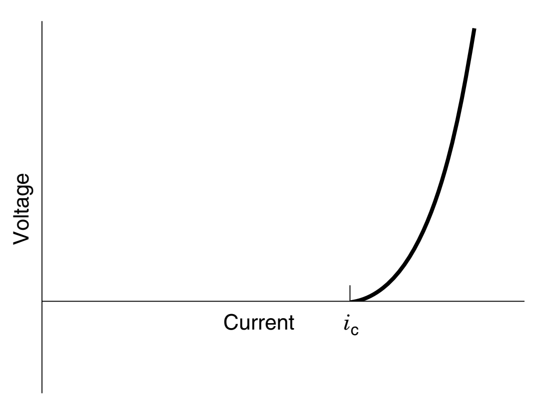

Figure 10. Voltage gradient along a composite superconductor as a function of steady current, showing the effect of index.

rent. The defined critical current is that at which a voltage gradient of, typically, 0.1 μV/cm is measured. As the current is increased beyond the critical value, that voltage gradient increases. An approximation to the gradient near to the critical current is

$$v \sim (i/i_c)^N \tag{19}$$

where i/i_c is the ratio of actual current to critical current and N is the index of the wire. The higher the value of N, the sharper is the superconducting to normal transition. Clearly, for values of i below the critical value, the voltage gradient will be small; the larger the index, the smaller the gradient. So, for NMR magnets, an appropriate combination of index and the ratio of i/i_c must be chosen. The index of most niobium–titanium (NbTi) wires suitable for MRI and NMR is typically 50. However, for niobium–tin (Nb_3Sn) wires, the index is lower, typically around 30, and the matrix is the more resistive bronze. So, for high field NMR magnets using Nb_3Sn inner sections, lower ratios of i/i_c are necessary. The concept of the index is only an approximation to the behavior of voltage as a function of current. In fact, theory and measurement indicate that the effective index increases as i/i_c decreases below 1 (15,16). Field decay arising from the index is constant and is distinguished from that caused by flux creep. The latter is a transient effect. It dies away with a logarithmic time dependence after a magnet has been set in persistent mode.

Protection of the magnet from the consequences of quenching must be compatible with the electrical and thermal isolation of the magnet from room temperature systems. Quenching is an spreading irreversible transition from the superconducting to the normal resistive state in the winding. The energy released during quenching in an NMR or MRI magnet must be dissipated as heat in the winding. In order to limit the energy and hence heat dissipated in any part of the winding, the magnet must be electrically divided into sections, each of which is provided with a shunt, often in the form of diodes. This subdivision limits the energy that can be transferred between sections and thereby minimizes the temperature rise and voltage generated within a section during quenching (17).

NMR Magnet Design

Figure 6 illustrates the winding array of a typical 750 MHz NMR magnet (18). Table 2 specifies the dimensions and winding specifications of the sections.

At a current of 307.86 A, these windings generate 17.616 T at the center; that corresponds to 750 MHz proton resonance frequency. The total inductance is 109.2 H, and the stored energy is 5.17 MJ. The first nonzero harmonic of the design is the 12th. The coils s, t, u, v, and w and their mirror images are the axial shim coils located in the annular space x. The radial shim coils are located in the space y.

The winding of the Nb_3Sn sections of high field NMR magnets presents particular problems. The wire is wound in the unreacted state after which it must be heated at about 700°C for up to 200 h to transform the separate niobium and tin components into the superconducting compound. The wire is insulated with S-glass braid, with a softening temperature of about 1000°C. (An alternative is E-glass. Although the E-glass may start to soften during the heat treatment, it is stronger in the prefired state than S-glass and therefore better survives the exigencies of winding.) After the heat treatment the winding is consolidated by impregnation with epoxy resin.

The forms on which the Nb_3Sn wire is wound must also endure the heat treatment without distortion. Stainless steel is the universal choice for the coil forms although titanium alloys have been used. The alloy 316 L is generally preferred because of its very small magnetic susceptibility. If the form is assembled with welds, those must be made with nonmagnetic filler, if used. The inner bore of the form must be quite thick if distortion is not to occur. The reason for that lies in the expansion coefficients of the wire and of stainless steel. The unreacted Nb_3Sn wire consists of bronze, niobium, tin, tantalum, and copper. During reaction, the copper and bronze have negligible strength, and the mechanical properties of the niobium and tantalum dominate. Their coefficients of thermal expansion are smaller than that of stainless steel with the consequence that, as the temperature rises during the heat treatment, the bore of the form will expand faster than the inner diameter of the winding. If the bore tube is thin, it can buckle against the constraint of the winding.

The need for thick bore tubes leads to windings of several wire diameters on one form. The thick bore tube occupies space that could otherwise be used by field-generating winding. In order to minimize the diluting effect of the bore tube, large winding builds are used. However, in the high field regions of Nb_3Sn windings, the wire diameter must be graded to optimize the cross section of Nb_3Sn corresponding to the local field. An alternative to the thick stainless steel bore tube is the transfer of the reacted winding to an aluminum form before impregnation with epoxy resin. This has been used occasionally, as in the example of Fig. 6 (18).

MRI Magnet Design

The design construction of MRI magnets follows the principles involved in the construction of NMR magnets (19). The forces and energies are generally greater. For example, the force tending to center each large end coil of the MRI magnet illustrated in Fig. 11 is 1,339,000 N (150 tons). NbTi conductor is used exclusively in MRI magnets because, to date, center fields of no more than 5 T are used. The NbTi filaments in the copper matrix of composite NbTi wires are twisted to approximate transposition. Because of the low fields in MRI magnets, wires with few NbTi filaments can be used. Those filaments can then be arrayed as a single circular layer within a copper matrix.The filaments are then fully transposed and are magnetothermally very stable. Mechanical perturbation is nevertheless a problem, and attention has to be paid to the interface between a winding and the coil form against which it presses. Because of the high stored energies, large copper cross sections are needed in the conductor to avoid over heating during quenching. Currents are typically up to 500 A. A common form of conductor is a composite wire embedded in a copper carrier. The latter frequently has a grooved rectangular cross section into which the composite wire is pressed or soldered. Insulation may be cotton or kapton wrap instead of enamel, and wax may be used as an impregnant as an alternative to epoxy.

Table 2. Dimensions of the Windings of a 700 MHz NMR Magnet

Section Number	Peak Field (T)	Wire Type	Wire Diameter (mm)	Inner Diameter (mm)	Outer Diameter (mm)	Winding Length (mm)	Number of Turns
a	17.62	Nb_3Sn	2.4	43	52.2	600	1000
b	16.97	Nb_3Sn	2.22	52.2	65.3	600	1620
c	15.93	Nb_3Sn	1.84	68.8	79.9	650	1770
d	14.8	Nb_3Sn	1.83	83.4	92.5	650	1780
e	13.83	Nb_3Sn	1.63	99.0	115.2	700	3870
f	11.80	Nb_3Sn	1.61	121.7	134.8	750	4194
g	9.83	NbTi	1.41	141.3	149.5	800	3396
h	8.31	NbTi	1.30	158.0	171.0	1000	6948
j	5.70	NbTi	1.14	176.0	186.2	1000	6992
k	3.13	NbTi	1.30	194.2	212.5	88.7	1020
l/*l*	3.14	NbTi	1.30	194.2	212.5	377.1	4110 (each)

At a current of 307.86 A these windings generate 17.616 T at the center; that corresponds to 750 MHz proton resonance frequency. The total inductance is 109.2 H and the stored energy is 5.17 MJ. The first nonzero harmonic of the design is the twelfth.

Most whole-body MRI magnets used in clinical applications have room temperature bores of between 1 and 1.3 m, with fields up to 2 T. An example of the profile of the windings of a whole-body MRI magnet is illustrated by the simple five-coil system of Fig. 11.

The center field is 1.5 T and the dimensions of the windings are listed in Table 3. The compensation is to tenth order (10 ppm over a 500 mm sphere). The current is 394 A for a 1.5 T center field. The inductance is 78 H and the stored energy 6 MJ.

The fringing field of this magnet extends a long way from the cryostat in which the coils are housed. The 1 mT (10 gauss) line is at an axial distance of 11.3 m and at a radial distance of 8.8 m from the center. Access to the space within these limits must be restricted because of the dangers to the wearers of pacemakers, the attraction of ferromagnetic objects, and the distortion of video monitors.

This may be an expensive restriction in a crowded hospital. Therefore, methods of shielding the space from the fringing fields are frequently used. Three methods are generally available: close iron, remote iron, and active shielding. The use of iron close to the coils has been used in a few instances. However, the iron must be at room temperature, to avoid otherwise severe cryogenic penalties. That leads to difficulties in balancing the forces between the coils and the iron in order to minimize the loads that the cryogenic supports must resist.

Remote iron takes the form of sheet, typically several millimeters thick, placed against the walls of the MRI room. This involves rather awkward architectural problems but is used frequently where the restricted space can still extend several meters from the cryostat.

The third form of shielding is by superconducting coils, built around the main coils, operating in series with the main coils as part of the persistent circuit, and in the same cryogenic environment. Those shield coils generate a reversed field to cancel, or reduce, the external fringing field. Typical of the resulting magnet is the eight-coil configuration shown schematically in Fig. 12.

Particular aspects of the illustration follow. The outwardly directed body forces in unshielded MRI windings are supported in tension in the conductor. However, in the shielded version, those forces are too large to be supported by the conductor alone, and a shell is applied to the outside of the winding against which the accumulated body forces act. Thus, the body forces on coils 3 and 4 are supported on their outer surfaces by a structural cylinder. Coil 4 provides the compensation of the dipole moment of the three inner windings so that the fringing fields of the magnet are much reduced from those of the unshielded magnet. The reduction in the volume of the restricted space is about 93%. The magnet is much heavier (and more expensive) than the simple unshielded type and the structural design of the cryostat and the suspension system is accordingly stronger. The highest fields generated at the center of shielded whole-body MRI magnets is 2 T. See also Ref. 12.

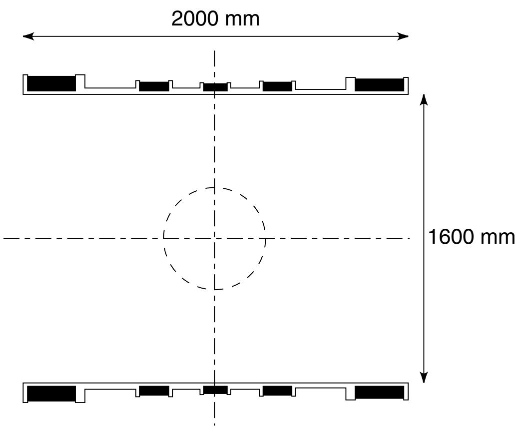

Figure 11. Coil profile of a 1.5 T unshielded MRI magnet illustrating typical coil placement.

Table 3. Example of a 1.5 T Whole-Body MRI Magnet

Coil Number	Inner Radius (mm)	Outer Radius (mm)	Left End (mm)	Right End (mm)	Number of Turns
1	741.9	807.1	−977.0	−724.9	3030
2	742.2	785.7	−391.9	−244.6	1180
3	742.1	777.0	−74.9	74.9	960
4	742.2	785.7	244.6	391.9	1180
5	741.9	807.1	724.9	977.0	3030

CRYOGENICS

As for NMR magnet systems, the economic operation of superconducting MRI magnets demands cryogenic systems with low heat in-leak. The evolution of MRI cryostats has been significant over the past 15 years. They have changed from simple liquid helium, liquid nitrogen shielded reservoirs with relatively high cryogen evaporation rates to single or multi-cryocooled cryostats. In one embodiment, no refrigerant is used in some types of cryocooled MRI magnets; in other examples, a combination of cryocoolers and refrigerants provide a zero evaporation rate. Demountable current leads are an essential feature of any magnet system with low refrigerant evaporation rate, and have been a standard feature of MRI magnet systems since 1974. An implication of demountable current leads is the need for the MRI magnet to be self-protecting during quenching, just as an NMR magnet must be.

PULSED GRADIENT COILS

In addition to the uniform background field, which it is the function of the MRI magnet to generate, pulsed gradient fields must be superimposed on that field in order to create the spatial encoding of the resonant frequencies of the protons (or other species) within the body. Those pulsed gradient fields are generated by three sets of room temperature coils, each set being driven by a powerful ramped current source. The pulsed field gradients are linear (dB/dz, dB/dx, dB/dy), as far as it is possible to design pure first-order gradient coils. Two problems arise in the overall design as a consequence of these pulsed gradient fields. The first is the effect on the superconductor of the periodic incident fields. Although the thermal shields and coil forms lie between the gradient coils and the superconductor, the incident pulsed field would still be significant there. Those small fields would cause a loss within the conductor through the mechanisms of hysteresis and coupling.

The second is the distortion of the gradients arising from currents induced in adjacent structures, such as the thermal shields and helium vessel, also sometimes the room temperature bore tube, if that is metallic. This distortion is minimized by locating sets of shield coils near the room temperature bore tube. These active shield coils are energized in opposition to the main pulsed gradient coils. They serve to confine the return flux of the gradient coils to flow in the space between the main gradient coils and the shield coils. The eddy currents induced in the surrounding structures are thereby minimized. The shield coils reduce the efficiency of the pulsed gradient system, that effect becoming more pronounced as the diameter of the main coils becomes a large fraction of that of the shield coils. At a diameter ratio greater than about 0.85, the efficiency is so reduced that the driving power required for useful gradient fields becomes prohibitively large. Figure 13 illustrates the form of the shielded dB/dx or dB/dy pulse coils. The dB/dZ coils are simple solenoids surrounded by shielding solenoids.

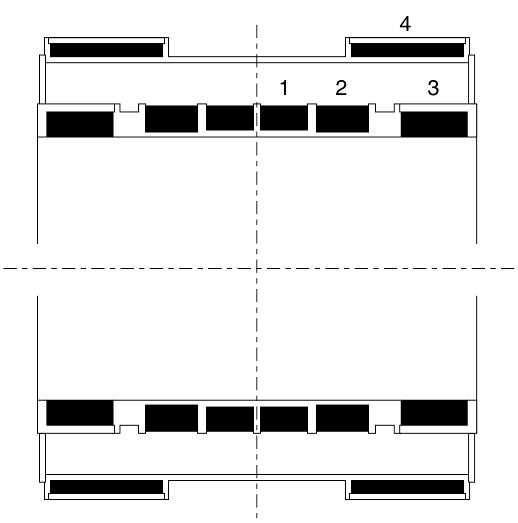

Figure 12. Schematic of an actively shielded MRI magnet showing the large coils needed to generate a main field while the shield coils generate an opposing field.

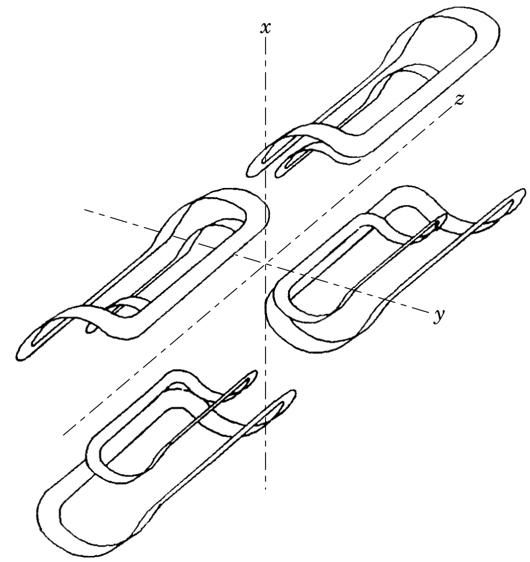

Figure 13. Schematic of actively shielded pulsed gradient coils for the dB_z/dx gradient showing the spacing between the main and shield coils.

BIBLIOGRAPHY

1. E. M. Purcell, H. C. Torrey, and R. V. Pound, Resonance absorption by nuclear magnetic moments in a solid, *Phys. Rev.,* **69**: 37, 1946.
2. F. Bloch, W. W. Hansen, and M. Packard, Nuclear induction, *Phys. Rev.,* **69**: 127, 1946.
3. E. Becker, *High resolution NMR, Theory and Applications,* New York: Academic Press, 1980.
4. R. R. Ernst, G. Bodenhausen, and A. Wokaun, *Principles of Nuclear Magnetic Resonance in One and Two Dimensions,* Oxford: Clarendon Press, 1987.
5. D. B. Montgomery, *Solenoid Magnet Design,* New York: Wiley-Interscience, 1969, p. 4.
6. M. D. Sauzade and S. K. Kan, High resolution nuclear magnetic spectroscopy in high magnetic fields, *Adv. Electron. Electron Phys.,* **34**: 1–93, 1973.
7. W. R. Smythe, *Static and Dynamic Electricity,* New York: McGraw-Hill, 1950, pp. 147–148.

8. M. Abramowitz and I. A. Stegun (eds.), *Handbook of Mathematical Functions,* Washington, DC: US Dept. of Commerce, Natl. Bur. of Standards, 1964.
9. F. Romeo and D. I. Hoult, Magnetic field profiling: Analysis and correcting coil design, *Magn. Resonance Med.,* **1**: 44–65, 1984.
10. M. R. Thompson, R. W. Brown, and V. C. Srivastava, An inverse approach to the design of MRI main magnetics, *IEEE Trans. Magn.,* **MAG-30**: 108–112, 1994.
11. W. H. Press et al., *Numerical Recipes: The Art of Scientific Computing,* Cambridge, UK: Cambridge Univ. Press, 1987.
12. F. J. Davies, R. T. Elliott, and D. G. Hawksworth, A 2 Tesla active shield magnet for whole body imaging and spectroscopy, *IEEE Trans. Magn.,* **MAG-27**: 1677–1680, 1991.
13. E. S. Bobrov and W. F. B. Punchard, A general method of design of axial and radial shim coils for NMR and MRI magnets, *IEEE Trans. Magn.,* **MAG-24**: 533–536, 1988.
14. P. Davis and P. Rabinowitz, Abscissas and weights for Gaussian quadrature of high order, *J. Res. NBS,* (RP2645), AMS (55): 35–37, 1956.
15. Y. Iwasa, *Case studies in Superconducting Magnets,* New York: Plenum, 1994, pp. 306–307.
16. J. E. C. Williams et al., NMR magnet technology at MIT, *IEEE Trans. Magn.,* **MAG-28**: 627–630, 1992.
17. B. J. Maddock and G. B. James, Protection and stabilisation of large superconducting coils, *Proc. Inst. Electr. Eng.,* **115**: 543–546, 1968.
18. A. Zhukovsky et al., 750 MHz NMR magnet development, *IEEE Trans. Magn.,* **MAG-28**: 644–647, 1992.
19. D. G. Hawksworth, Superconducting magnets systems for MRI, *Int. Symp. New Develop. in Appl. Superconductivity,* Singapore: World Scientific, 1989, pp. 731–744.

JOHN E. C. WILLIAMS
Massachusetts Institute of Technology

MAGNETS FOR NMR. See MAGNETS FOR MAGNETIC RESONANCE ANALYSIS AND IMAGING.

MAGNETS, PERMANENT. See PERMANENT MAGNETS.

MAGNETS, SUPERCONDUCTING. See SUPERCONDUCTING CRITICAL CURRENT; SUPERCONDUCTING MAGNETS FOR PARTICLE ACCELERATORS AND STORAGE RINGS; SUPERCONDUCTING MAGNETS, QUENCH PROTECTION.

MAGNETS, SUPERCONDUCTING FOR NUCLEAR FUSION. See SUPERCONDUCTING MAGNETS FOR FUSION REACTORS.

MAINTENANCE, AIRCRAFT. See AIRCRAFT MAINTENANCE.

MAINTENANCE, JET TRANSPORT AIRCRAFT. See JET TRANSPORT MAINTENANCE.

MAINTENANCE, SOFTWARE. See SOFTWARE MAINTENANCE.